

**RECENT DEVELOPMENTS IN PERTURBATIVE QCD:
 Q^2 EVOLUTION OF CHIRAL-ODD DISTRIBUTIONS
 $h_1(x, Q^2)$ and $h_L(x, Q^2)$ ^a**

YUJI KOIKE

*Graduate School of Science and Technology, Niigata University
 Ikarashi, Niigata 950-21, Japan
 E-mail: koike@nt.sc.niigata-u.ac.jp*

After reviewing QCD definitions of the chiral-odd spin-dependent parton distributions $h_1(x, Q^2)$ and $h_L(x, Q^2)$, I will summarize the main feature of the recent two results in perturbative QCD: (i) Next-to-leading order Q^2 evolution of $h_1(x, Q^2)$. (ii) Leading order Q^2 evolution of the twist-3 distribution $h_L(x, Q^2)$ and the universal simplification of the Q^2 evolution of all the twist-3 distributions in the large N_c limit.

1 Introduction

Recent developments in collider experiments have been providing us with rich information on the quark-gluon distributions in the nucleon. Particularly interesting are the spin structure functions which reveal “spin distributions” carried by quarks and gluons inside the nucleon. Besides the importance in their own right, they play an indispensable role to test the spin-dependent part of QCD – fundamental theory of the strong interaction: Deeper test of QCD in the spin dependent level may eventually lead us to search for a new physics beyond the standard model.

The nucleon’s structure functions measured in hard processes can be written as a sum of parton distributions for each quark or anti-quark flavor and a gluon. They are functions of Bjorken’s x which represent parton’s momentum fraction in the nucleon and a scale Q^2 at which they are measured. Until now, most data on the nucleon’s structure functions have been obtained through the lepton-nucleon deep inelastic scattering (DIS). The chiral-odd distributions, $h_{1,L}(x, Q^2)$, however, can not be measured by the inclusive DIS, and hence there has been no data up to now. They can be measured by the nucleon-nucleon polarized Drell-Yan process and semi-inclusive DIS which detect particular hadrons in the final state. They will hopefully be measured by planned experiments using polarized accelerators at BNL, DESY, CERN and SLAC etc¹. In particular, RHIC at BNL is expected to provide first data on these distributions.

^aInvited talk presented at “QCD Corrections and the New Physics”, October 27-29, 1997, Hiroshima, Japan. To be published in the proceedings. (ed. by J. Kodaira et al.)

In the study of these structure functions, perturbative QCD plays an indispensable role in predicting their Q^2 -dependence: Given a structure function, say $h_1(x, Q_0^2)$, at one scale Q_0^2 , perturbative QCD predicts the shape of $h_1(x, Q^2)$ at an arbitrary scale Q^2 . This Q^2 evolution is necessary not only in extracting low energy hadron properties from high energy experimental data but also in testing the x -dependence predicted by a non-perturbative QCD technique or a model with the high energy data. In this talk, I will first give the QCD definition of $h_{1,L}(x, Q^2)$ and discuss their Q^2 -dependence studied in the recent literature.

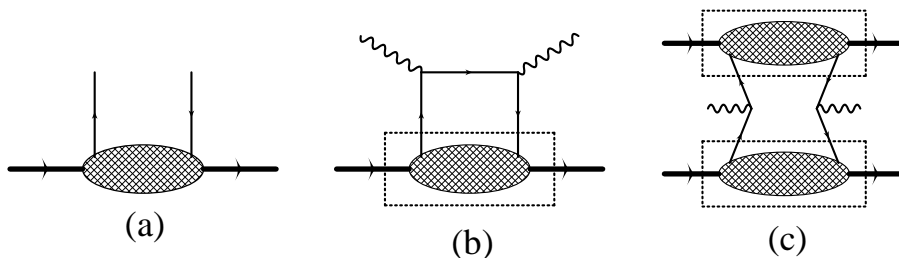


Figure 1: (a) Quark distribution function. (b) Nucleon structure function in DIS. (c) Cross section for the nucleon-nucleon Drell-Yan process.

2 Chiral-Odd Distributions $h_{1,L}(x, Q^2)$

Inclusive hard processes can be generally analyzed in the framework of the QCD factorization theorem². This theorem generalizes the idea of the Bjorken-Feynman’s “parton model” and allows us to include QCD correction in a systematic way. Here I restrict myself to the hard processes with the nucleon target, such as lepton-nucleon deep inelastic scattering (DIS, $l + p \rightarrow l' + X$), Drell-Yan ($p + p' \rightarrow l^+ l^- + X$), semi-inclusive DIS ($l + p \rightarrow l' + h + X$). According to the above theorem, the cross section (or the nucleon structure function) for these processes can be factorized into a “soft part” and a “hard part”: The soft part represents the parton (quark or gluon) distribution in the nucleon and the hard part describes the short distance cross section between the parton and the external hard probe which is calculable within perturbation theory. For example, a nucleon structure function in DIS can be written as the imaginary part of the virtual photon-nucleon forward Compton scattering amplitude. (Fig. 1 (b)) According to the above theorem, in the Bjorken limit, i.e. $Q^2, \nu = P \cdot q \rightarrow \infty$ with $x = Q^2/2\nu = \text{finite}$, ($Q^2 = -q^2$ is the virtuality of the space-like photon, P is the nucleon’s four momentum), the structure

function can be written as

$$W(x, Q^2) = \sum_a \int_x^1 \frac{dy}{y} H^a\left(\frac{x}{y}, \frac{Q^2}{\mu^2}, \alpha_s(\mu^2)\right) \Phi^a(y, \mu^2), \quad (1)$$

where Φ^a represents a distribution of parton a in the nucleon and H^a describes the short distance cross section of the parton a with the virtual photon. μ^2 is the factorization scale. In Fig. 1(b), Φ^a is identified by the dotted line. (Fig.1 (a)). Similarly to DIS, the cross section for the nucleon-nucleon Drell-Yan process can also be written in a factorized form at $s = (P_A + P_B)^2$, $Q^2 \rightarrow \infty$ with a fixed Q^2/s ($P_{A,B}$ are the momenta of the two nucleons, Q is the momentum of the virtual photon):

$$d\sigma \sim \sum_{a,b} \int_{x_a}^1 dy_a \int_{x_b}^1 dy_b H^{ab}\left(\frac{x_a}{y_a}, \frac{x_b}{y_b}, Q^2; \frac{Q^2}{\mu^2}, \alpha_s(\mu^2)\right) \Phi^a(y_a, \mu^2) \Phi^b(y_b, \mu^2) \quad (2)$$

where the two parton distributions, Φ^a and Φ^b , for the beam and the target appear as was shown by dotted lines in Fig. 1(c).

As is seen from Figs. 1(b),(c), the parton distribution can be regarded as a parton-nucleon forward scattering amplitude shown in Fig. 1 (a) which appear in several different hard processes. In particular, the quark distribution in the nucleon moving in the $+\hat{e}_3$ direction can be written as the light-cone Fourier transform of the quark correlation function in the nucleon:³

$$\Phi^a(x, \mu^2) = P^+ \int_{-\infty}^{\infty} \frac{dz^-}{2\pi} e^{ixP \cdot z} \langle PS | \bar{\psi}^a(0) \Gamma \psi^a(z) |_{\mu} PS \rangle, \quad (3)$$

where $|PS\rangle$ denotes the nucleon (mass M) state with momentum P^μ and spin S^μ , and ψ^a is the quark field with flavor a . In (3), we have suppressed for simplicity the gauge link operator which ensures the gauge invariance and $|_{\mu}$ indicates the operator is renormalized at the scale μ^2 . A four vector a^μ is decomposed into two light-cone components $a^\pm = \frac{1}{\sqrt{2}}(a^0 \pm a^3)$ and the transverse component \vec{a}_\perp . In (3), $z^+ = 0$, $\vec{z}_\perp = \vec{0}$, and $z^2 = 0$. Γ generically represents γ -matrices, $\Gamma = \gamma_\mu, \gamma_\mu \gamma_5, \sigma_{\mu\nu}, 1$. $\Phi^a(x, \mu^2)$ measures the distribution of the parton a to carry the momentum $k^+ = xP^+$ in the nucleon, which is independent from particular hard processes.

If one puts $\Gamma = \gamma_\mu, \gamma_\mu \gamma_5$, the chirality of $\bar{\psi}$ and ψ becomes the same, namely it defines the chiral-even distributions. Likewise, putting $\Gamma = \sigma_{\mu\nu}, 1$ defines the chiral-odd distributions. For the case of the deep-inelastic scattering (Fig. 1 (b)), the quark line emanating from the target nucleon comes back to the original nucleon after passing through the hard interactions. Since the

perturbative interaction in the standard model preserves the chirality except a tiny quark mass effect, the chirality of the two quark lines entering the nucleon in Fig. 1(b) is the same. Hence the DIS can probe only the chiral-even quark distributions. On the other hand, in the Drell-Yan process (Fig. 1 (c)), there is no correlation in chirality between two quark lines entering each nucleon. Therefore the Drell-Yan process probes both chiral even and odd distributions.

The chiral-odd distributions $h_1^a(x, \mu^2)$, $h_L^a(x, \mu^2)$ in our interest are defined by putting $\Gamma = \sigma_{\mu\nu}i\gamma_5$ in (3):⁴

$$\begin{aligned}
P^+ \int \frac{dz^-}{2\pi} e^{ixP \cdot z} \langle PS | \bar{\psi}^a(0) \sigma_{\mu\nu} i\gamma_5 \psi^a(z) |_{\mu} | PS \rangle \\
= 2[h_1^a(x, \mu^2)(S_{\perp\mu}p_\nu - S_{\perp\nu}p_\mu)/M \\
+ h_L^a(x, \mu^2)M(p_\mu n_\nu - p_\nu n_\mu)(S \cdot n) \\
+ h_3^a(x, \mu^2)M(S_{\perp\mu}n_\nu - S_{\perp\nu}n_\mu)]
\end{aligned} \tag{4}$$

where we introduced two light-like vectors p , n ($p^2 = n^2 = 0$) by the relation $P^\mu = p^\mu + \frac{M^2}{2}n^\mu$, $p \cdot n = 1$, $p^- = n^+ = 0$. If we write $P^+ = \mathcal{P}$, $p = \frac{\mathcal{P}}{\sqrt{2}}(1, 0, 0, 1)$, $n = \frac{1}{\sqrt{2}\mathcal{P}}(1, 0, 0, -1)$. \mathcal{P} is a parameter which specifies the Lorentz frame of the system: $\mathcal{P} \rightarrow \infty$ corresponds to the infinite momentum frame, and $\mathcal{P} \rightarrow M/\sqrt{2}$ the rest frame of the nucleon. S_\perp^μ is the transverse component of S^μ defined by $S^\mu = (S \cdot n)p^\mu + (S \cdot p)n^\mu + S_\perp^\mu$. One can show that Φ^a defined in (3) has a support $-1 < x < 1$. If one replaces the quark field ψ in (3) by its charge conjugation field $C\bar{\psi}^T$, it defines the anti-quark distribution $\bar{\Phi}^a$. In particular $h_{1,L,3}^a(x, \mu^2)$ in (4) are related to their anti-quark distribution by $h_{1,L,3}^a(-x, \mu^2) = -\bar{h}_{1,L,3}^a(x, \mu^2)$.

Φ^a appears in a physical cross section in the form of the convolution with a short distance cross section in a parton level as is shown in (1) and (2). The cross section can be expanded in powers of $\frac{1}{\sqrt{Q^2}}$ as

$$\sigma(Q^2) \sim A(\ln Q^2) + \frac{M}{\sqrt{Q^2}}B(\ln Q^2) + \frac{M^2}{Q^2}C(\ln Q^2) + \dots, \tag{5}$$

where each coefficient A , B , C receives logarithmic Q^2 -dependence due to the QCD radiative correction. In order to see how $h_{1,L,3}$ can contribute in the expansion (5), it is convenient to move into the infinite momentum frame ($\mathcal{P} \sim Q \rightarrow \infty$). In this limit the coefficient of $h_{1,L,3}$ in (4) behaves, respectively, as $O(Q)$, $O(1)$, $O(1/Q)$. Therefore if h_1 contributes to the A term in (5), h_L can contribute at most to the B -term, and h_3 can contribute at most to the C -term. In general, when a distribution function contributes to hard processes at

spin	average	longitudinal	transverse
twist-2	f_1	g_1	$\underline{h_1}$
twist-3	\underline{e}	$\underline{h_L}$	g_T

Table 1: Classification of the quark distributions based on spin, twist and chirality. Underlined distributions are chiral-odd. Others are chiral-even.

most in the order of $\left(\frac{1}{\sqrt{Q^2}}\right)^{\tau-2}$, the distribution is called twist- τ . Therefore h_1, h_L, h_3 in (4) is, respectively, twist-2, -3 and -4.

Twist-2 distribution h_1 can be measured through the transversely polarized Drell-Yan^{5,6,4,7}, semi-inclusive deep inelastic scatterings which detect pion⁸, polarized baryons^{6,9,10}, correlated two pions¹¹.

From the discussion above, one sees that it is generally difficult to isolate experimentally higher twist ($\tau \geq 3$) distributions in hard processes, since they are hidden by the leading twist-2 contribution (A term in (5)). However, this is not the case for h_L and g_T . In particular spin asymmetries, they contribute to the B -term in the absence of A -term: g_T can be measured in the transversely polarized DIS¹², and h_L appears in the longitudinal versus transverse spin asymmetry in the polarized nucleon-nucleon Drell-Yan process⁴. Therefore the Q^2 -evolution of g_T and h_L can be a new test of perturbative QCD beyond the twist-2 level.

Insertion of other γ -matrices in (3) defines other distributions. In Table 1, we show the classification of the quark distributions up to twist-3.⁴ There $f_1, g_{1,T}, e$ is defined, respectively, by $\Gamma = \gamma_\mu, \gamma_\mu\gamma_5, 1$ in (3). A similar classification can also be extended to the gluon distributions¹⁴. The distribution f_1 contributes to the spin averaged structure functions $F_{1,2}(x, Q^2)$ familiar in DIS. The helicity distribution g_1 contributes to the $G_1(x, Q^2)$ structure function measured in the longitudinally polarized DIS. By now there has been much accumulation of experimental data on f_1 and g_1 , and the data on g_1 triggered lots of theoretical discussion on the ‘‘origin of the nucleon spin’’¹. The first nonzero data on $g_2 (= g_T - g_1)$ was also reported in Ref.¹³.

3 Next-to-leading order (NLO) Q^2 -evolution of $h_1(x, Q^2)$

As we saw in the previous section, h_1 is the third and the final twist-2 quark distribution. It has a simple parton model interpretation as can be seen by the Fourier expansion of ψ in (4). It measures the probability in the transversely polarized nucleon to find a quark polarized parallel to the nucleon spin minus the probability to find it oppositely polarized. Here the transverse polarization

refers to the eigenstate of the transverse Pauli-Lubański operator $\gamma_5 \not{S}_\perp$. If one replaces the transverse polarization by the longitudinal one, it becomes the helicity distribution g_1 . For nonrelativistic quarks, $h_1(x, \mu^2) = g_1(x, \mu^2)$. A model calculation suggests, h_1 is the same order as g_1 .^{4,15,16}

The Q^2 -evolution of h_1 is described by the usual DGLAP evolution equation¹⁷. Because of its chiral-odd nature it does not mix with gluon distributions. Therefore the Q^2 -dependence of h_1 is described by the same equation both for singlet and nonsinglet distributions. For f_1 and g_1 , the NLO Q^2 evolution was derived long time ago^{18,19,20,21} and has been frequently used for the analysis of experiments^{22,23}. The leading order (LO) Q^2 -evolution for h_1 has been known for some time⁶. In the recent literature, the next-to-leading order (NLO) Q^2 -evolution has been completed by two papers^{24,25} almost at the same time: Vogelsang²⁴ presented the light-cone gauge calculation for the two-loop splitting function of h_1 in the formalism originally used for f_1 ²⁰. We²⁵ carried out the Feynman gauge calculation of the two-loop anomalous dimension following the method of Ref. ¹⁸ for f_1 . The results of these calculations in the $\overline{\text{MS}}$ scheme agreed completely. This result was subsequently confirmed by Ref. ²⁷. In the following, I briefly discuss the characteristic feature of the NLO Q^2 evolution of h_1 following Refs.^{25,26}.

Analysis of (4) gives the connection between the n -th moment of h_1 and a tower of twist-2 operators:

$$\begin{aligned} \mathcal{M}_n[h_1(\mu^2)] &\equiv \int_{-1}^1 dx x^n h_1(x, \mu^2) = \frac{-1}{2M} \langle PS_\perp | O_n^\nu(\mu^2) S_{\perp\nu} | PS_\perp \rangle, \\ O_n^\nu &= \bar{\psi} \sigma^{\nu\alpha} n_\alpha i \gamma_5 (in \cdot D)^n \psi, \end{aligned} \quad (6)$$

where S_\perp stands for the transverse polarization and $O_n^\nu(\mu^2)$ indicates the operator O_n^ν is renormalized at the scale μ^2 . The contraction with n^μ and S_\perp^μ (recall $S_\perp \cdot n = 0$, $n^2 = 0$) in (6) projects out the relevant twist-2 contribution from the composite operator. (“Twist” for local composite operators is defined as dimension minus spin.) By solving the renormalization group equation for $O_n^\nu S_{\perp\nu}$, one gets the NLO Q^2 dependence of $\mathcal{M}_n[h_1(\mu^2)]$ as

$$\frac{\mathcal{M}_n[h_1(Q^2)]}{\mathcal{M}_n[h_1(\mu^2)]} = \left(\frac{\alpha_s(Q^2)}{\alpha_s(\mu^2)} \right)^{\gamma_n^{(0)}/2\beta_0} \left[1 + \frac{\alpha_s(Q^2) - \alpha_s(\mu^2)}{4\pi} \frac{\beta_1}{\beta_0} \left(\frac{\gamma_n^{(1)}}{2\beta_1} - \frac{\gamma_n^{(0)}}{2\beta_0} \right) \right], \quad (7)$$

where $\alpha_s(Q^2)$ is the NLO QCD running coupling constant given by

$$\frac{\alpha_s(Q^2)}{4\pi} = \frac{1}{\beta_0 \ln(Q^2/\Lambda^2)} \left[1 - \frac{\beta_1 \ln \ln(Q^2/\Lambda^2)}{\beta_0 \ln(Q^2/\Lambda^2)} \right], \quad (8)$$

with the one-loop and two-loop coefficients of the β -function $\beta_0 = 11 - 2/3N_f$ and $\beta_1 = 102 - 38/3N_f$ (N_f is the number of quark flavor) and the QCD scale parameter Λ . $\gamma_n^{(0)}$ and $\gamma_n^{(1)}$ are the one-loop and two-loop coefficients of the anomalous dimension γ_n for $O_n^\nu S_{\perp\nu}$ defined as

$$\gamma_n = \frac{\alpha_s}{4\pi} \gamma_n^{(0)} + \left(\frac{\alpha_s}{4\pi}\right)^2 \gamma_n^{(1)} + \dots \quad (9)$$

If one sets $\beta_1 \rightarrow 0$ and $\gamma_n^{(1)} \rightarrow 0$ in (7), the leading order (LO) Q^2 evolution is obtained. $\gamma_n^{(0)}$ and $\gamma_n^{(1)}$ are obtained, respectively, by calculating the one-loop and two-loop corrections to the two-point Green function which imbeds $O_n^\nu S_{\perp\nu}$. To obtain $\gamma_n^{(1)}$, calculation of 18 two-loop diagrams is required in the Feynman gauge. Since the expression for $\gamma_n^{(1)}$ is quite complicated, we refer the readers to Refs. ^{24,25} for them.

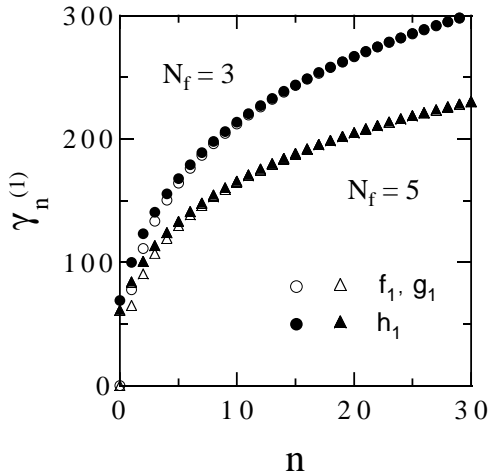


Figure 2: The NLO anomalous dimension $\gamma_n^{h(1)}$ in comparison with $\gamma_n^{fg(1)}$. This figure is taken from Ref. ²⁵.

In order to get a rough idea about the NLO Q^2 dependence of h_1 , we plotted in Fig. 2 $\gamma_n^{h(1)}$ ($\gamma_n^{(1)}$ for h_1) in comparison with $\gamma_n^{fg(1)}$ ($\gamma_n^{(1)}$ for the nonsinglet f_1 and g_1) for $N_f = 3, 5$. One sees from Fig. 2 $\gamma_n^{h(1)} > \gamma_n^{fg(1)}$ especially at small n . This suggests that the NLO Q^2 evolution of h_1 is quite different from that of f_1 and g_1 in the small x region. The relation $\gamma_n^{h(1)} > \gamma_n^{fg(1)}$ is in parallel with and even more conspicuous than the LO anomalous

dimensions which read

$$\begin{aligned}\gamma_n^{h^{(0)}} &= 2C_F \left(1 + 4 \sum_{j=2}^{n+1} \frac{1}{j} \right), \\ \gamma_n^{fg^{(0)}} &= 2C_F \left(1 - \frac{2}{(n+1)(n+2)} + 4 \sum_{j=2}^{n+1} \frac{1}{j} \right).\end{aligned}\quad (10)$$

To illustrate the generic feature of the Q^2 evolution, we have applied the obtained Q^2 evolution to a reference distribution for g_1 and h_1 . As a reference distribution, we take GRSV g_1 distribution²³ and assume $h_1(x, \mu^2) = g_1(x, \mu^2)$ at a low energy input scale ($\mu^2 = 0.23 \text{ GeV}^2$ for LO and $\mu^2 = 0.34 \text{ GeV}^2$ for NLO evolution) as is suggested by a nucleon model^{4,15}. We then evolve them to $Q^2 = 20 \text{ GeV}^2$ and see how much deviation is produced between them. The result is shown in Fig. 3. As is expected from the anomalous dimension, the drastic difference in the Q^2 evolution between h_1 and g_1 is observed in the small x region, and this tendency is more significant for the NLO evolution.^{28,29,26} (Although g_1 for u -quark mixes with the gluon distribution, the same tendency in the difference from h_1 is observed for the nonsinglet distribution.)

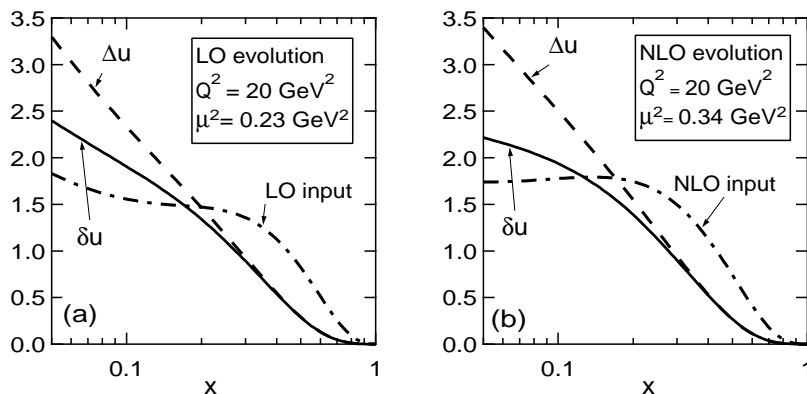


Figure 3: (a) The LO Q^2 evolution of h_1 (denoted by δu) and g_1 (denoted by Δu) for the u -quark. (b) The NLO Q^2 evolution of h_1 and g_1 for the u -quark. This figure is taken from Ref. ²⁶

As another example, we showed in Fig.4 the Q^2 evolution of the tensor

charge (Fig. 4(a)) and the first moment of h_1 and the nonsinglet f_1 (g_1) (Fig. 4(b)). Although the NLO effect is sizable for the tensor charge, it is small for the first moment. (For the lattice QCD calculation of the tensor charge, see Ref. ³⁰.)

In Ref. ³¹, the Regge asymptotics of h_1 was studied and the small- x behavior was predicted to be $h_1(x) \sim \text{constant}$ ($x \rightarrow 0$). On the other hand, the rightmost singularity of $\gamma_n^{h(0)}$ and $\gamma_n^{h(1)}$ are, respectively, located at $n = -2$ and $n = -1$ in the complex n plane. Therefore inclusion of the NLO effect in the DGLAP asymptotics gives consistent behavior at $x \rightarrow 0$ as the Regge asymptotics. This is in contrast to the (nonsinglet) f_1 and g_1 distributions, whose LO and NLO DGLAP asymptotics are the same.

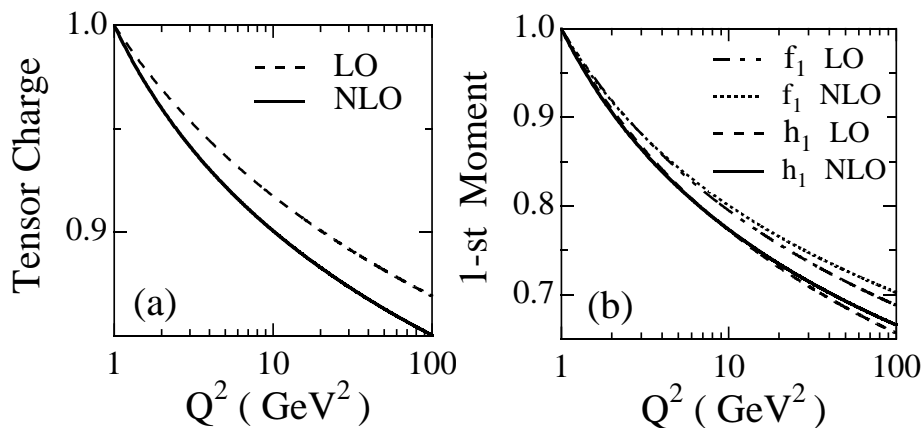


Figure 4: (a) The LO and NLO Q^2 evolution of the tensor charge normalized at $Q^2 = 1$ GeV^2 . (b) The LO and NLO Q^2 evolution of the first moment of h_1 and the nonsinglet f_1 (or g_1). This figure is taken from Ref. ²⁵.

One of the interesting applications of the obtained NLO Q^2 evolution of h_1 is the preservation of the Soffer's inequality;³² $2|h_1^a(x, Q^2)| \leq f_1^a(x, Q^2) + g_1^a(x, Q^2)$. Although the validity of this inequality hinges on schemes beyond LO³³, the NLO Q^2 evolution maintains the inequality at $Q^2 > Q_0^2$ if it is satisfied at some (low) scale Q_0^2 in suitably defined factorization schemes such as $\overline{\text{MS}}$ and Drell-Yan factorization schemes.^{34,24}

As was discussed in Sec. 2, a physical cross section is a convolution of a parton distribution and a short distance cross section. (See (1) and (2)) For the double transverse spin asymmetry (A_{TT}) in the Drell-Yan process, the NLO

short distance cross section has been calculated in Ref. ³⁵ in the $\overline{\text{MS}}$ scheme. The analysis on A_{TT} combined with the NLO transversity distribution predicts modest but not negligible NLO effect.³⁶

4 Q^2 -evolution of $h_L(x, Q^2)$ and its $N_c \rightarrow \infty$ limit

In general, higher twist ($\tau \geq 3$) distributions represent quark-gluon correlation in the nucleon. Using the QCD equation of motion, one obtains from (4) the following relation³⁷:

$$h_L(x, \mu^2) = 2x \int_x^1 \frac{dy}{y^2} h_1(y, \mu^2) + \tilde{h}_L(x, \mu^2), \quad (11)$$

$$\tilde{h}_L(x, \mu^2) = \frac{iP^+}{M} \int_{-\infty}^{\infty} \frac{dz^-}{2\pi} e^{-2ixP \cdot z} \int_0^1 u du \int_{-u}^u t dt$$

$$\times \langle PS_{\parallel} | \bar{\psi}(uz) i\gamma_5 \sigma_{\mu\alpha} g G_{\nu}^{\alpha}(tz) z^{\mu} z^{\nu} \psi(-uz) | PS_{\parallel} \rangle, \quad (12)$$

where $z^2 = 0$, $z^+ = 0$ and S_{\parallel} stands for the longitudinal polarization for the nucleon ($S^{\mu} = S_{\parallel}^{\mu} = p^{\mu} - \frac{M^2}{2} n^{\mu}$). This equation means that h_L consists of the twist-2 contribution and \tilde{h}_L which represents quark-gluon correlation in the nucleon. We call the latter contribution ‘‘purely twist-3’’ contribution. (Expansion of (12) produces twist-3 local operators. See (15) below.) Equation (11) reminds us of the Wandzura-Wilczek relation³⁸ for g_T :

$$g_T(x, \mu^2) = \int_x^1 \frac{dy}{y} g_1(y, \mu^2) + \tilde{g}_T(x, \mu^2). \quad (13)$$

For e and \tilde{g}_T , one can write down relations similar to (12).

The Q^2 -evolution of the first and second terms in (11) is described separately. The evolution of \tilde{h}_L is quite complicated. A detailed analysis of (12) leads to the following relation for the n -th moment of \tilde{h}_L ⁴:

$$\mathcal{M}_n[\tilde{h}_L(\mu^2)] = \sum_{k=2}^{[(n+1)/2]} \left(1 - \frac{2k}{n+2}\right) \frac{1}{2M} \langle PS_{\parallel} | R_{nk}(\mu) | PS_{\parallel} \rangle, \quad (14)$$

$$R_{nk} = \frac{1}{2} [\bar{\psi} \sigma^{\lambda\alpha} n_{\lambda} i\gamma_5 (in \cdot D)^{k-2} i g G_{\nu\alpha} n^{\nu} (in \cdot D)^{n-k} \psi - (k \rightarrow n - k + 2)]. \quad (15)$$

We note that the number of independent operators $\{R_{nk}\}$ ($k = 2, \dots, [(n+1)/2]$) increases with n . In the Q^2 -evolution, the mixing among $\{R_{nk}\}$ occurs and the renormalization is described by the anomalous dimension matrix

$[\gamma_n(g)]_{kl}$ for $\{R_{nk}\}$. If we put the LO anomalous dimension matrix for $\{R_{nk}\}$ as $[\gamma_n(g)]_{kl} = (\alpha_s/2\pi)[X_n]_{kl}$ corresponding to (9), the solution to the renormalization group equation for $\{R_{nk}\}$ takes the following matrix form:

$$\langle PS_{\parallel}|R_{nk}(Q^2)|PS_{\parallel}\rangle = \sum_{l=2}^{[(n+1)/2]} \left[L^{X_n/\beta_0} \right]_{kl} \langle PS_{\parallel}|R_{nl}(\mu^2)|PS_{\parallel}\rangle, \quad (16)$$

where $L \equiv \frac{\alpha_s(Q^2)}{\alpha_s(\mu^2)}$. X_n for \tilde{h}_L was derived in Ref. ³⁹. The Q^2 -evolution for \tilde{g}_T and e is also described by matrix equation similar to (16), and the solution was obtained in Refs.^{40,41} for g_T and in Ref.⁴² for e .⁴³ As is clear from (14) and (16) $\mathcal{M}_n[\tilde{h}_L(Q^2)]$ and $\mathcal{M}_n[\tilde{h}_L(\mu^2)]$ are not connected by a simple equation as in the case for the twist-2 distribution (see (7)).⁴⁴ Although (16) gives complete prediction for the Q^2 evolution, it is generally difficult to distinguish contribution from many operators in the analysis of experiments.

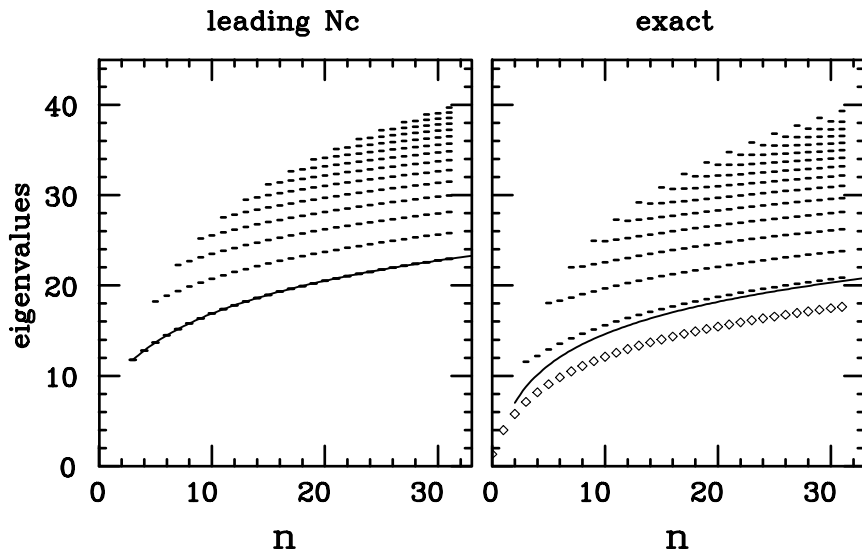


Figure 5: (Right) Complete spectrum of the eigenvalues of the anomalous dimension matrix for \tilde{h}_L obtained in Ref. ³⁹. The symbol \diamond denotes the one-loop anomalous dimension for h_1 . The solid line is the anomalous dimension (21) at large n . (Left) Spectrum of the eigenvalues of the anomalous dimension matrix for \tilde{h}_L at large N_c . The solid line denotes the analytic solution given in (18). This figure is taken from Ref. ³⁷.

In order to get some feeling on the Q^2 -evolution of \tilde{h}_L , we plotted the eigenvalues of X_n in Fig. 5 (right). For comparison, we also showed in the

same figure the LO anomalous dimension $\gamma_n^{(0)}/2$ for h_1 . (Note the difference in convention between (7) and (16).) As is clear from this figure, the Q^2 evolution of \tilde{h}_L is much faster than that of h_1 . (See discussion below.)

In the recent literature^{45,37,42}, it has been shown that at large N_c (the number of colors), a great simplification occurs in the Q^2 -evolution of the twist-3 distributions. Recall X_n in (16) is a function of two Casimir operators $C_G = N_c$ and $C_F = \frac{N_c^2-1}{2N_c}$. If one takes $N_c \rightarrow \infty$, i.e. $C_F \rightarrow N_c/2$, (14) and (16) is reduced to

$$\mathcal{M}_n[\tilde{h}_L(Q^2)] = L^{\tilde{\gamma}_n^h/\beta_0} \mathcal{M}_n[\tilde{h}_L(\mu^2)], \quad (17)$$

$$\tilde{\gamma}_n^h = 2N_c \left(\sum_{j=1}^n \frac{1}{j} - \frac{1}{4} + \frac{3}{2(n+1)} \right). \quad (18)$$

This evolution equation is just like those for the twist-2 distributions (see (7)). In Fig. 5 (left), we showed the distribution of the eigenvalues of X_n obtained numerically at $N_c \rightarrow \infty$. The solid line is the analytic solution in (18), which shows (18) corresponds to the lowest eigenvalues at $N_c \rightarrow \infty$. Since (17) was obtained by a mere replacement $C_F \rightarrow N_c/2$ in (16), the correction to the result is of $O(1/N_c^2) \sim 10\%$ level, which gives enough accuracy for practical applications.

This large- N_c simplification is a consequence of the fact that the coefficients of R_{nk} in (14) constitutes the *left* eigenvector of X_n corresponding to the eigenvalue $\tilde{\gamma}_n^h$ in this limit:

$$\sum_{k=2}^{[(n+1)/2]} \left(1 - \frac{2k}{n+2} \right) [X_n]_{kl} = - \left(1 - \frac{2l}{n+2} \right) \tilde{\gamma}_n^h, \quad (19)$$

which implies that all the *right* eigenvectors of X_n except the one corresponding to $\tilde{\gamma}_n^h$ are orthogonal to the vector consisting of $\left(1 - \frac{2k}{n+2} \right)$. This leads to (17).

This large- N_c simplification of the Q^2 evolution was proved for the nonsinglet \tilde{g}_T in Ref.⁴⁵ and for \tilde{h}_L and e in Ref.³⁷. The corresponding anomalous dimensions for \tilde{g}_T and e are, respectively,

$$\begin{aligned} \tilde{\gamma}_n^g &= 2N_c \left(\sum_{j=1}^n \frac{1}{j} - \frac{1}{4} + \frac{1}{2(n+1)} \right), \\ \tilde{\gamma}_n^e &= 2N_c \left(\sum_{j=1}^n \frac{1}{j} - \frac{1}{4} - \frac{1}{2(n+1)} \right). \end{aligned} \quad (20)$$

Corresponding to three twist-3 distributions in table 1, there are three independent twist-3 fragmentation functions.⁹ (Their number is doubled to 6 if one includes final state interactions. See Ref.⁹) It has been shown in Ref.⁴⁶ that at large N_c the Q^2 evolution of all these nonsinglet fragmentation functions is also described by a simple evolution equation similar to (17). Therefore the simplification of the twist-3 evolution equation is universal to all twist-3 nonsinglet distribution and fragmentation functions.

To illustrate the actual Q^2 evolution of h_L , we have applied (17) to the bag model calculation of h_L .⁴⁷ (Fig. 6) Fig. 6(a) shows the bag calculation of h_L .⁴ At the bag scale, purely twist-3 contribution \tilde{h}_L is comparable to the twist-2 contribution. After the Q^2 evolution to $Q^2 = 10 \text{ GeV}^2$, h_L is dominated by the twist-2 contribution. This is a consequence of the large anomalous dimension (18) compared with the LO anomalous dimension of h_1 (\diamond in the right figure of Fig. 5). A similar calculation was done for g_T in Ref.⁴⁸.

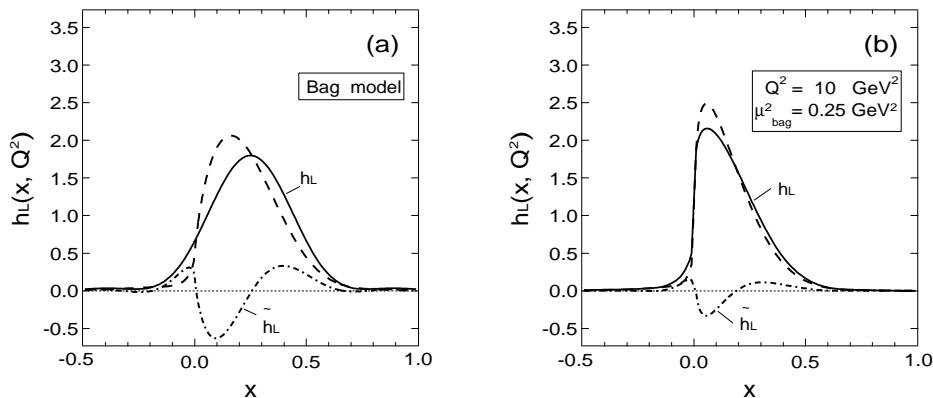


Figure 6: (a) Bag model prediction for h_L . The dashed line represents the twist-2 contribution to h_L . (b) Bag model prediction for h_L evolved to $Q^2 = 10 \text{ GeV}^2$ assuming the bag scale is $\mu^2 = 0.25 \text{ GeV}^2$. These figures are taken from Ref.⁴⁷

Another simplification of the twist-3 evolution occurs at $n \rightarrow \infty$.^{45,37} In this limit, all the twist-3 distributions obey a simple DGLAP equation (17) with a common anomalous dimension which is slightly shifted from (18) and (20):

$$\gamma_n = 4C_F \left(\sum_{j=1}^n \frac{1}{j} - \frac{3}{4} \right) + N_c. \quad (21)$$

This evolution equation satisfies the complete evolution equation to the $O(\ln(n)/n)$ accuracy⁴⁵. In the right figure of Fig. 5, (21) is shown by the solid line. One sees that it is close to the lowest eigenvalues except for small n . Combined with this $n \rightarrow \infty$ result, the large- N_c evolution equation in (17) with (18) and (20) for each distribution is valid to $O((1/N_c^2)\ln(n)/n)$ accuracy.

5 Summary

In this talk, I discussed the recent progress in perturbative QCD, especially the Q^2 evolution of the chiral-odd spin-dependent parton distributions $h_1(x, Q^2)$ and $h_L(x, Q^2)$.

The NLO Q^2 evolution for the transversity distribution $h_1(x, Q^2)$ was completed in the $\overline{\text{MS}}$ scheme. This means the Q^2 evolution of all the twist-2 distributions has been understood in the NLO level. The resulting Q^2 evolution of $h_1(x, Q^2)$ turned out to cause quite different behavior from the helicity distribution $g_1(x, Q^2)$ in the small x region if h_1 is assumed to be equal to g_1 at a low energy scale.

The LO Q^2 evolution for the twist-3 distribution $h_L(x, Q^2)$ (and $e(x, Q^2)$) was completed. Although their Q^2 evolution is quite complicated due to the mixing among increasing number of quark-gluon-quark operators, it obeys a simple DGLAP equation similar to the twist-2 distribution in the $N_c \rightarrow \infty$ limit, as was the case for the Q^2 evolution of the nonsinglet $g_T(x, Q^2)$ distribution. The same simplification at $N_c \rightarrow \infty$ was also proved for the twist-3 fragmentation functions. Therefore this large- N_c simplification was proved to be universal for the twist-3 distribution and fragmentation functions.

By these studies, we now have at hand the necessary tools given by perturbative QCD for the analysis of the whole parton distributions. From the point of view of the “spin distributions” in the nucleon, one is more interested in the nonperturbative x dependence of those parton distributions. Armed with the development in the perturbative Q^2 dependence and the nonperturbative QCD techniques, we will be forced to challenge this issue when the new spin colliders start producing data on the new spin distributions.

Acknowledgements

I would like to thank I.I. Balitsky, V.M. Braun, A. Hayashigaki, Y. Kanazawa, N. Nishiyama and K. Tanaka for the collaboration on which this talk is based. I'm also grateful to J. Kodaira for inviting me to such an exciting conference.

References

1. See, for example, *Spin Structure of the Nucleon* (World Scientific, 1996, eds. T.-A. Shibata et al.); *SPIN96* (World Scientific, 1997, eds. C.W. de Jager et al.).
2. J.C. Collins, D. Soper and G. Sterman, in *Perturbative Quantum Chromodynamics* (World Scientific, Singapore, 1989, ed. A.H. Mueller), and references quoted therein.
3. J.C. Collins and D.E. Soper, Nucl. Phys. **194**, 445 (1982).
4. R.L. Jaffe and X. Ji, Nucl. Phys. **B375**, 527 (1992).
5. J.P. Ralston and D.E. Soper, Nucl. Phys. **B152**, 109 (1979).
6. X. Artru and M. Mekhfi, Z. Phys. **C45** 669 (1990); Nucl. Phys. **A532** (1991) 351c.
7. J.L. Cortes, B. Pire and J.P. Ralston, Z. Phys. **C55**, 409 (1992).
8. R.L. Jaffe and X. Ji, Phys. Rev. Lett **71**, 2547 (1993).
9. X. Ji, Phys. Rev. **D49**, 114 (1994).
10. R.L. Jaffe, Phys. Rev. **D54**, 6581 (1996).
11. R.L. Jaffe, X. Jin and J. Tang, hep-ph/9709322.
12. R.L. Jaffe, Comm. Nucl. Part. Phys. **19**, 239 (1990).
13. The Spin Muon Collaboration (D. Adams et al.), Phys. Lett. **B336**, 125 (1994); E143 Collaboration (K. Abe et al.), Phys. Rev. Lett. **76**, 587 (1996).
14. A.V. Manohar, Phys. Rev. Lett. **65**, 2511 (1990); **66**, 289 (1991); X. Ji, Phys. Lett. **B289**, 137 (1992).
15. P.V. Pobylitsa and M.V. Polyakov, Phys. Lett. **B389**, 350 (1996); V. Barone, T. Calarco and A. Drago, Phys. Lett. **B390**, 287 (1997).
16. For a review on h_1 , see R.L. Jaffe, hep-ph/9710465, to be published in Proc. of 2nd Topical Workshop on Deep Inelastic Scattering off Polarized Targets: Theory Meets Experiment (DESY-Zeuthen, Sep. 1-5, 1997).
17. V.N. Gribov and L.N. Lipatov, Sov. J. Nucl. Phys. **15**, 438 (1972), G. A. Altarelli and G. Parisi, Nucl. Phys. **B126**, 298 (1977), Yu. L. Dokshitzer, Sov. Phys. JETP **46**, 641 (1977).
18. E.G. Floratos, D.A. Ross and C.T. Sachrajda, Nucl. Phys. **B129**, 66 (1977); **B139**, 545 (1978) (E); Nucl. Phys. **B152**, 493 (1979).
19. A. Gonzalez-Arroyo, C. Lopez and F.J. Yndurain, Nucl. Phys. **B153**, 161 (1979).
20. G. Curci, W. Furmanski and R. Petronzio, Nucl. Phys. **B175**, 27 (1980), W. Furmanski and R. Petronzio, Phys. Lett **97B**, 437 (1980).
21. R. Mertig, W.L. van Neerven, Z. Phys. **C70** 637 (1996); W. Vogelsang, Phys. Rev. **D54** 2023 (1996).
22. M. Glück, E. Reya and A. Vogt, Z. Phys. **C53**, 127 (1992); A.D. Martin, W.J. Stirling and R.G. Roberts, Phys. Lett. **B354**, 155 (1995); H.L.

- Lai, et. al. Phys. Rev. **D51**, 4763 (1995).
23. M. Glück, E. Reya, M. Stratmann and W. Vogelsang, Phys. Rev. **D53**, 4775 (1996); T. Gehrmann and W.J. Stirling, Phys. Rev. **D53**, 6100 (1996); G. Altarelli, R. Ball, S. Forte and G. Ridolfi, Nucl. Phys. **B496**, 337 (1997).
 24. W. Vogelsang, hep-ph/9706511, to appear in Phys. Rev. **D**.
 25. A. Hayashigaki, Y. Kanazawa and Y. Koike, Phys. Rev. **D56**, 7350 (1997).
 26. A. Hayashigaki, Y. Kanazawa and Y. Koike, hep-ph/9710421, to be published in Proc. of 2nd Topical Workshop on Deep Inelastic Scattering off Polarized Targets: Theory Meets Experiment (DESY-Zeuthen, Sep. 1-5, 1997).
 27. S. Kumano and M. Miyama, Phys. Rev. **D56**, 2504 (1997). Revised after submission. See also comment [10] of Ref. ²⁶.
 28. V. Barone, T. Calarco and A. Drago, Phys. Rev. **D56**, 527 (1997).
 29. S. Scopetta and V. Vento, hep-ph/9707250.
 30. S. Aoki, M. Doui, T. Hatsuda and Y. Kuramashi, Phys. Rev. **D56**, 433 (1997).
 31. R. Kirschner, L. Mankiewicz, A. Schäfer and L. Szymanowski, Z. Phys. **C74**, 501 (1997); R. Kirschner, hep-ph/9710253, to be published in Proc. of 2nd Topical Workshop on Deep Inelastic Scattering off Polarized Targets: Theory Meets Experiment (DESY-Zeuthen, Sep. 1-5, 1997).
 32. J. Soffer, Phys. Rev. Lett. **74**, 1292 (1995).
 33. G.R. Goldstein, R.L. Jaffe and X. Ji, Phys. Rev. **D52**, 5006 (1995).
 34. C. Bourrely, J. Soffer and O.V. Teryaev, hep-ph/9710224.
 35. A.P. Contogouris, B. Kamal and Z. Merebashvili, Phys. Lett. **B337**, 169 (1994); B. Kamal, Phys. Rev. **D53**, 1142 (1996).
 36. O. Martin, A. Schäfer, M. Stratmann, and W. Vogelsang, hep-ph/9710300.
 37. I.I. Balitsky, V.M. Braun, Y. Koike and K. Tanaka, Phys. Rev. Lett. **77**, 3078 (1996).
 38. W. Wandzura and F. Wilczek, Phys. Lett. **B72**, 195 (1977).
 39. Y. Koike and K. Tanaka, Phys. Rev. **D51**, 6125 (1995).
 40. E.V. Shuryak and A.I. Vainshtein, Nucl. Phys. **B201**, 141 (1982); A.P. Bukhvostov, E.A. Kuraev and L.N. Lipatov, Sov. Phys. JETP **60**, 22 (1984). P.G. Ratcliffe, Nucl. Phys. **B264**, 493 (1986); I.I. Balitsky and V.M. Braun, Nucl. Phys. **B311**, 541 (1988/89); X. Ji and C. Chou, Phys. Rev **D42**, 3637 (1990); D. Müller, Phys. Lett. **B407**, 314 (1997).
 41. J. Kodaira, Y. Yasui and T. Uematsu, Phys. Lett. **B344**, 348 (1995); J. Kodaira, Y. Yasui, K. Tanaka and T. Uematsu, Phys. Lett. **B387**,

- 855 (1996); J. Kodaira, T. Nasuno, H. Tochimura, K. Tanaka, Y. Yasui, hep-ph/9712395, Prog. Theor. Phys. in press.
42. Y. Koike and N. Nishiyama, Phys. Rev. **D55**, 3068 (1997).
 43. In carrying out the renormalization of the twist-3 distributions in the covariant gauge, there arises complication due to the mixing with an equation-of-motion (EOM) operator and a BRS exact operator as well as “alien” operators in the intermediate step. For this point and a method to handle the issue, see Refs. ^{39,41}.
 44. For the evolution equation for h_L and e , see A.V. Belitsky and D. Müller, Nucl. Phys. **B503**, 279 (1997).
 45. A. Ali, V.M. Braun and G. Hiller, Phys. Lett. **B266**, 117 (1991).
 46. A.V. Belitsky, Phys. Lett. **B312**, 312 (1997); A.V. Belitsky and E.A. Kuraev, Nucl. Phys. **B499**, 301 (1997).
 47. Y. Kanazawa and Y. Koike, Phys. Lett. **B403**, 357 (1997).
 48. M. Stratmann, Z. Phys. **C60**, 763 (1993).